STRUCTURAL DAMAGE DETECTION USING CHAOTIC TIME SERIES EXCITATION

Lillian Y. Chang [1], Karl A. Erickson [2], Kenton G. Lee [3], Michael D. Todd [4]

[1] Dept. of Mechanical Engineering, Stanford University, Stanford, CA 94309 (lillian.chang@stanford.edu)
[2] Dept. of Electrical Engineering, University of California, Los Angeles, CA 90024 (ekarl@ucla.edu)
[3] Dept. of Aerospace Engineering, Embry-Riddle Aeronautical University, Prescott, AZ 86301 (leeke@erau.edu)
[4] Structural Engineering Department, UC San Diego, M/C 0085, La Jolla, CA 92093-0085 (mdt@ucsd.edu)

ABSTRACT

This study explores a structural damage detection strategy employing the novel use of chaotic time series excitation. Chaotic time series have several useful properties such as determinism and controllable dimension. Therefore, these series are attractive candidates for probing a structure's dynamics for the subtle changes that could occur because of damage. This approach is applied to a metal frame structure connected by bolted joints. Under loading, fatigue damage causes the pre-loads in the bolts to lessen, leading to an increasing inability of the joint to accommodate design loads. This project explores the use of propagating chaotic waveforms through the frame structure and to determine a diagnostic parameter that reflects the structural health of the bolted joints. Analysis of vibration response to chaotic input is used to detect the extent and location of pre-load loss. Using the cross-prediction error as a feature for damage detection was successful in identifying damage and, using excitation to response prediction errors, locating damage. However, in other cross comparisons of attractors, the prediction error was not able to locate the damage. In addition, the extent of damage was not correlated with the magnitude of prediction error.

NOMENCLATURE

N	dimension of a system
x, $x(t)$	a time-dependent variable corresponding to a degree of freedom in the system
$x^{(N)}$	the N^{th} derivative of x
T	time delay for attractor reconstruction
m	embedding dimension of attractor
x,y,z	three coordinates describing the degrees of the system of the Lorenz attractor
μ	global mean of the resampled data subsets
$Z_{\alpha/2}$	standard normal deviate associated with 95% confidence
σ	global standard deviation of the resampled subsets
n	size of each resampled subset

I. INTRODUCTION

The ability to detect structural damage is vital to the maintenance of any mechanical system. With an increasing trend toward reducing maintenance personnel for large mechanical systems such as naval vessels, methods to detect and locate damage must be implemented to compensate for personnel reduction. Structural health monitoring (SHM) seeks to extend the operational lifetime of a structure and prevent structural failures, which are often catastrophic. The usual steps in SHM are to identify damage, estimate the extent of damage, locate the damage, and predict the remaining life of the structure. This study focuses on the diagnosing the presence, extent, and location of damage rather than the prognosis of future performance of the structure. A variety of SHM techniques exist to identify damage using non-destructive operational evaluation and feature extraction.

Traditional acoustic approaches for structural health monitoring usually use broadband, stochastic excitation. For example, modal-based techniques focus on the transient response of the structure, which is characterized by its damping and mode shapes. Other techniques focus on the steady state response to ambient excitation. An overview of vibration-based techniques is provided in [1]. The drawback of an acoustic modal approach is that the steady state response of a structure to a wide-bandwidth excitation is often too high-dimensional for reliable interpretation of damage conditions. On the other extreme, response to purely sinusoidal input is too low-dimensional to allow observable changes in the system's dynamic response. However, by using chaotic excitation interrogation of a structure, the steady state response is both high-dimensional enough to reflect the dynamic range of the structure's health conditions and low-dimensional enough for calculation of a reliable feature diagnostic.

Chaotic excitation methods have been shown to be capable of detecting bolt pre-load loss through comparison of a structure's changing response to a deterministic input signal at different damage conditions. Previous studies [2,3,4] used the auto-prediction error of an attractor reconstructed from sensor responses as a feature to diagnose the extent of damage to the structure. Other work using chaotic excitation examined instead the cross-prediction error between pairs of sensor responses in order to estimate both extent and location of damage [4]. This study uses similar data acquisition and cleansing techniques to calculate cross-prediction error to diagnose damage of an aluminum frame structure. Section II, Method of Approach, provides a more detailed background of the techniques for analyzing chaotic dynamics.

Because large mechanical systems often have thousands of bolted joints to clamp surfaces together, this study focuses on the loss of preload in bolted joints by examining the structure's response to a chaotic time series excitation. Varying the pre-load tension in a bolt changes the integrity of the particular joint and also changes the structure's global dynamic properties. The damaged frame structure then responds differently to the same chaotic input, in this case, the Lorenz attractor. Section III describes the laboratory procedure for controlling damage to the frame structure, cleansing data, and calculating cross prediction errors.

Out of the three objectives to identify, estimate extent of, and locate damage, the cross-prediction error approach used with the test structure could only identify and, in selected channel cross-relationships, locate damage. Section IV and V discuss the results of the study and make recommendations for further investigation of the cross-prediction error method as a damage detection strategy.

II. NONLINEAR CROSS-PREDICTION ERROR METHOD

This section outlines the damage detection strategy used by reviewing chaotic dynamics and attractor-based analysis. Analysis of a time series in phase space reveals useful topographic features of the data. However, practical reconstruction of an attractor from experimental data requires careful choice of parameters for the delay coordinate approach. Once attractors have been reconstructed from response time series, the cross-prediction error of two attractors is a feature used to compare the relationship between the two time series. More detailed explanations of nonlinear time series analyses are provided in References [2-5].

A. Attractors and phase space orbit trajectories

Consider a system of ordinary differential equations with N degrees of freedom, with each coordinate being a different function of the system's state:

$$\begin{aligned} \dot{x}_1 &= F_1(\vec{x}, \dot{\vec{x}}) \\ \dot{x}_2 &= F_2(\vec{x}, \dot{\vec{x}}) \\ &\vdots \\ \dot{x}_N &= F_N(\vec{x}, \dot{\vec{x}}) \end{aligned} \tag{1}$$

where $x_1, x_2, \ldots x_N$ are the N coordinates of the system, and $F_1, F_2, \ldots F_N$ are the state functions describing the system. The solution to this system traces out a unique path in an N-dimensional space [6]. For any system with dissipative qualities (true for all real structures), the trajectory will eventually collapse onto a lower-dimensional response than the full phase space. If the system is stable, the trajectory will return to this same orbit even if the system is perturbed. This *attractor* thus describes the steady state behavior of the system (see Figure 1).

The trajectory describing a system with multiple degrees of freedom has certain geometric properties such that viewing a system's response in phase space form reveals information about the structure otherwise missed by other modal-based and/or transient techniques. Attractors describing structural response to purely sinusoidal input are often one-dimensional. However, because of the controllable dimension of chaos, using a chaotic waveform to interrogate the structure will result in higher-dimensional attractors that are still low-enough dimension for robust calculations.

Specifically, the Lorenz attractor is a three dimensional system described by the system of equations:

$$\begin{aligned} \dot{x} &= q(y - x) \\ \dot{y} &= -xz + rx - y \\ \dot{z} &= xy - bz \end{aligned} \tag{2}$$

where x, y, z are the three coordinates of the system, and q, r, b are constants. Because the Lorenz attractor is well-understood and has been used in previous studies as the input excitation [2-5], this project will use the *x* coordinate of the Lorenz attractor as the chaotic waveform used to interrogate the structure. (See Section IIIA on Experimental Procedure.) The Lorenz system was first inspired by weather modeling research and is sensitive to small changes in initial parameters [7]. Because the Lorenz attractor has a low dimension of three, it is useful for chaotic interrogation to control the dimensionality of the structural response.

Using time series techniques to analyze the phase space response of a structure to chaotic input allows varying damage conditions to be observable in the geometry of the constructed attractor.

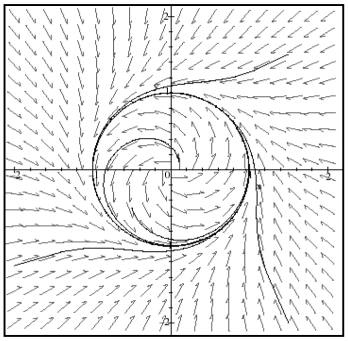

Figure 1. A limit cycle is an example of a one-dimensional attractor.

B. Attractor reconstruction using delay coordinate approach

In theory, an attractor in phase space is an *N*-dimensional trajectory constructed from a time series *x* and its successive *N*-1 time rates of change. In practice, it is often difficult to directly and completely measure all of the degrees of freedom for a given structural system. It is useful to instead qualitatively reconstruct a topologically equivalent attractor with a delay coordinate approach [8]. This idea, known as Taken's theorem, is powerful because it implies that the dynamic properties of a system of *x* and its continuous derivatives are completely captured in a qualitative sense by the time series *x* alone [9]. Thus, attractor reconstruction of a measured laboratory system is possible from a single discrete time series response. This transformation is useful because computerized data acquisition systems record discrete rather than continuous time signals.

The delay coordinate approach [10] successively shifts the original time series *x* in place of directly measuring or continuously differentiating to find its time-derivatives. Two essential parameters are the time delay *T* and the embedding dimension *m*, which respectively describe how many time steps and for how many times the signal is recursively shifted. Using this technique, an attractor represented in phase space by $x, x', x'', \ldots x^{(N)}$ is reconstructed from $x(t), x(t+T), x(t+2T), \ldots x(t+(m-1)T)$. Figure 2 shows an example of the original Lorenz attractor and the attractor with equivalent topology that was reconstructed by embedding the coordinate *x.*

A variety of algorithms exist for choosing appropriate values for the delay and embedding dimension so that each shifted time signal is neither redundant nor completely independent [11]. Many methods select the delay *T* as the time for which the time series is least correlated with itself, either when the auto-correlation function of the signal is a minimum, a zero, or below a threshold percent [2,12,13]. Similarly, the dimension *m* is chosen when the number of 'false nearest neighbors' [11] is a minimum or below a threshold such that the attractor is unambiguously unfolded in *m*-dimensional phase space.

For a monitored system, a number of attractors can be reconstructed from sensor signals describing the structure's dynamic response at various locations. The properties of the reconstructed attractors can be compared by computing a parameter called the prediction error.

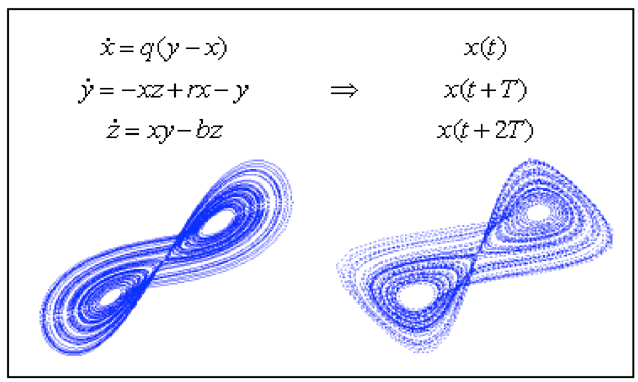

Figure 2. Left, the original Lorenz attractor plotted from numerical solutions of *x, y,* and z from the system of equations. Right, the Lorenz attractor reconstructed using the delay coordinate approach to embed the coordinate *x*.

C. Comparing attractors with cross-prediction error

As a structure's health degrades, the relative dynamics of system's local regions change. Accordingly, the attractors reconstructed from sensor signals at various locations have different topologies for the range of damage conditions. In particular, as pre-load tension in a bolted joint decreases, the response of the parts in the vicinity become decoupled.

The cross-prediction error is one metric that describes the relationship between attractors representing two time series [10,12]. This approach was originally developed to detect time series nonstationarity [14] but adapted algorithms have been used in other work for structural health monitoring [2-5]. Similar to the method used in [5], this study uses the cross-prediction error as an extracted feature for damage detection.

Using the prediction error method focuses on the ability of related topological points to predict the future location of the trajectory. Given a random fiducial point on one trajectory, a specified number of points in the

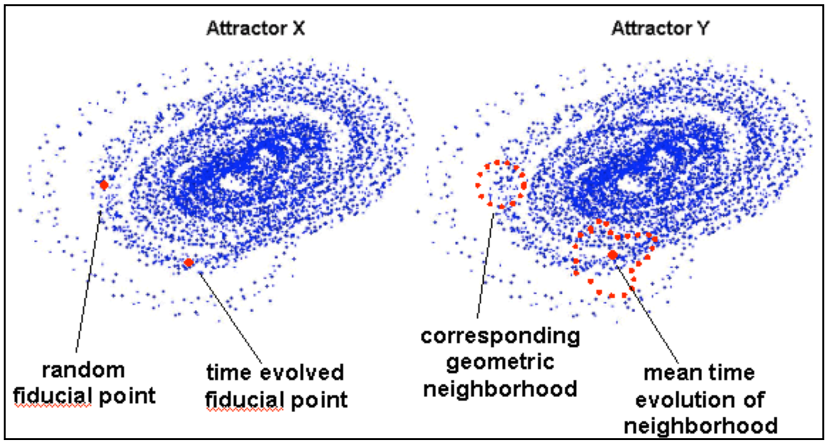

Figure 3. A qualitative illustration of the cross prediction error between two attractors. The prediction error is the Euclidean distance between the time evolved fiducial point and the geometric center of the evolved neighborhood in a second attractor.

corresponding geometric neighborhood on the other trajectory are selected. Both the single point and the neighborhood of points are advanced a small number of time steps. Comparing the geometric center of the evolved group of points to the actual destination of the single point indicates how well the second trajectory can predict the first. The Euclidean distance between the single advanced point and the center of the evolved neighborhood is the prediction error. Figure 3 illustrates the concept behind the cross-prediction approach.

Both cross-prediction error reflecting how one attractor predicts another and a self-prediction error representing how one trajectory predicts itself can be used as metrics to monitor a system. Coupling between each sensor signal changes as the structure is damaged such that local responses are less correlated, resulting in higher prediction errors. This study focuses on the cross-prediction error of attractors constructed from accelerometer responses as a feature to describe the damage conditions of a bolted structure.

III. PROCEDURE

A. Experimental Setup

The apparatus for the experiment included an aluminum frame structure (see Figure 4) and electrodynamic shaker both clamped to a workbench. The structure was clamped to simulate a fixed boundary condition. The fixed boundary condition was chosen because the low frequency bias of the Lorenz waveform resulted in the entire structure being translated as a rigid body by the shaker input under free boundary conditions. All bolts in the frame were torqued to 68 N-m except the instrumented bolt.

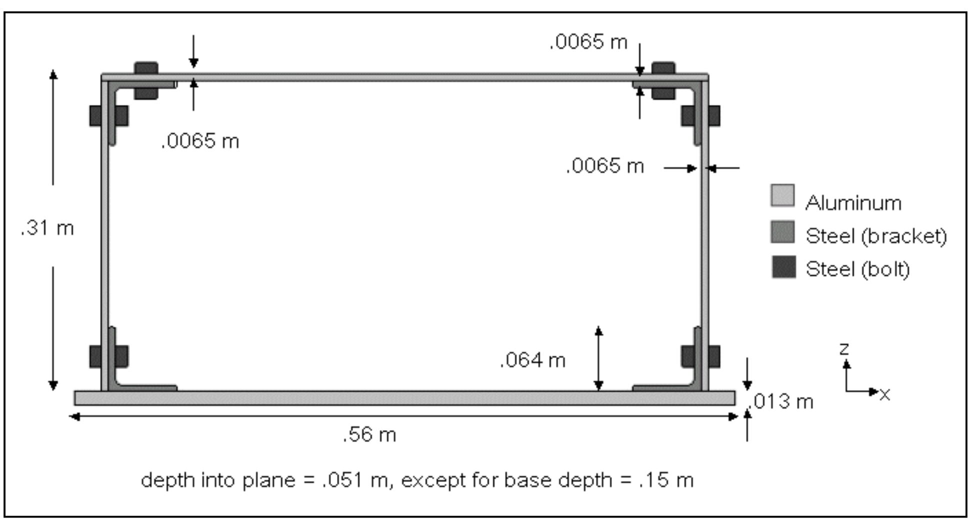

Figure 4. The aluminum frame used as the test structure consisted of base, two side beams, and one top beam connected by steel angle brackets and steel bolts.

A power amplifier transferred the Lorenz waveform signal to the shaker, which in turn delivered force to the structure in the horizontal direction via a stinger with a PCB 208-A03 force transducer, designated channel (Ch) 1, mounted to the structure. Four accelerometers were used to measure the response of the system at locations near the joints. One PCB 355B04 1 V/g accelerometer, designated channel 2, was mounted in the horizontal direction just below the shaker input connection and another was mounted vertically on the top beam just left of the upper right bracket, designated channel 3. One PCB 352A24 100 mV/g accelerometer, designated channel 4 was mounted horizontally on the left side of the upper right bracket and another, designated channel 5 was mounted horizontally on the right vertical beam just below the upper right bracket (see Figure 5).

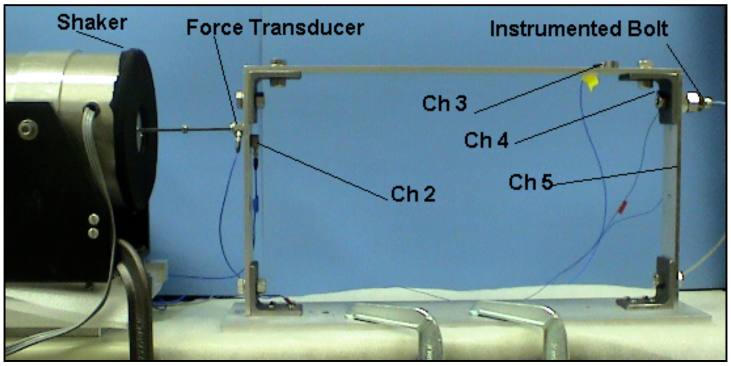

Figure 5. Instrumentation of the frame structure included coupling with a horizontal shaker stinger rod, a force transducer (channel 1) to measure the stinger input into the structure, four accelerometers to measure the structure's response at various locations (channels 1-4), and an instrumented bolt at the damaged joint (channel 6).

The top right bracket was connected to the right vertical beam (as shown in Figure 6) using an ALD-DYNAGAGE instrumented bolt, which was connected to a 10V DC power supply for the wheatstone bridge excitation. The power amplifier, force transducer, accelerometers, and instrumented bolt were connected to a National Instruments data acquisition board with BNC connectors. The data acquisition board was connected to a desktop PC with a National Instruments 6052E data acquisition card. The experiment was controlled by a laptop computer, which was connected via Ethernet to the desktop PC. MATLAB 6.5 was used extensively in both the data acquisition and data analysis phases of the study with MATLAB's xPC Target toolbox being the primary software component for data acquisition. The laptop was the host computer for xPC Target, and the desktop PC was the target computer.

For the first test condition, the instrumented bolt was left fully loose so that there was a visible gap between the nut and the structure. Executing a MATLAB script started the shaker with the Lorenz waveform input for 25 seconds. The second before and after the shaker run were also recorded for the purpose of monitoring the preload in the bolt under static conditions. Five runs were recorded under this condition and then the bolt was tightened to the next test condition. Table 1 summarizes the bolt preload conditions tested.

Table 1. Experimental Damage Conditions

Damage Case	Description	Measured Bolt Preload (N)
1	27 N-m torque	10400
2	14 N-m torque	7860
3	7 N-m torque	6420
4	3 N-m torque	5450
5	1 N-m torque	4780
6	Finger tight	4550
7	Loose no gap	--
8	Loose with gap	--

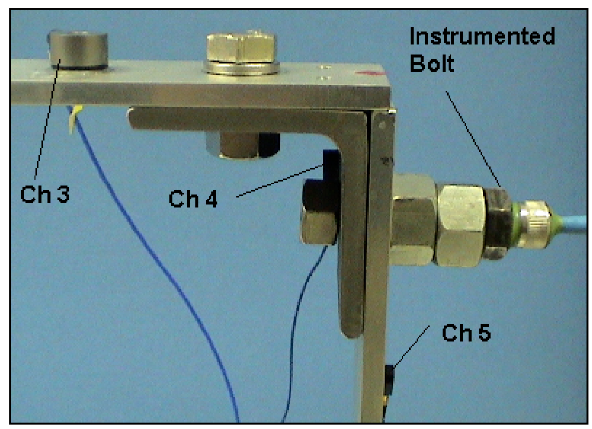

Figure 6. A detailed view of the instrumented structure shows the horizontal bolt connection which was damaged (loosened) during testing. The instrumented bolt recorded the tension, while accelerometers on the steel angle bracket (channel 4) and the right side beam (channel 5) measure signals across the joint.

Representative time series data for the Lorenz waveform signal and the corresponding time series responses of the force transducer and accelerometers are shown in Figure 7. The output from sensors located close to the shaker input are more similar to the original Lorenz waveform than those from more remote sensors because of structural filtering.

B. Data Acquisition and Cleansing

Processing the experimental data was accomplished with a combination of MATLAB scripts and TISEAN routines. TISEAN is a set of executable programs written in C for non-linear time series analysis [15]. The first step in processing the data was to remove 0.25 s from both the beginning and end of the run to eliminate any transients from the shaker starting and stopping. The delay was chosen as the point at which TISEAN's autocorrelation function showed the time series was less than 33 percent correlated with itself. Finding the embedding dimension was accomplished with TISEAN's false nearest neighbors function by finding the dimension where the function decayed below 5 percent or its first minimum. Representative plots of the results of the autocorrelation and false nearest neighbors functions are shown in Figure 8.

After determining the delay and embedding dimension, the cross prediction error between the time series measured by different accelerometers was calculated using a version of TISEAN's xzero function that had been modified to pick a random fiducial point. For the eight damage conditions, 1000 cross prediction errors were calculated for the Ch 4 attractor predicting the Ch 5 attractor and 1000 for the Ch 5 attractor predicting the Ch 4 attractor. Both prediction directions were examined to see if the predictions were direction independent. The choice of calculating 1000 prediction errors was made to adequately compare the attractor topologies. Additionally, cross prediction errors in both directions were calculated for the force transducer predicting each of the accelerometer responses as well as Ch 2 predicting Ch 4 and Ch 5 responses.

After the cross prediction errors had been calculated, the results were resampled. The algorithm generated a new set of data by randomly selecting 50 points with replacement from the original data set and calculating the mean. This process was repeated 1000 times for each damage condition to generate a set of resampled data. Confidence limits were defined by two-sided hypothesis testing of the mean. The data were thus plotted as the global resampled mean bounded by the upper and lower confidence limits:

$$\mu \pm \frac{Z_{\alpha/2}\,\sigma}{\sqrt{n}} \tag{3}$$

where μ is the global mean of the resampled subsets, $Z_{\alpha/2}$ = 1.96 is the standard normal deviate associated with 95% confidence, σ is the global standard deviation of the resampled subsets, and n = 50 is the size of each subset. Such a procedure, under the central limit theorem, converges the probability density function to a Gaussian profile.

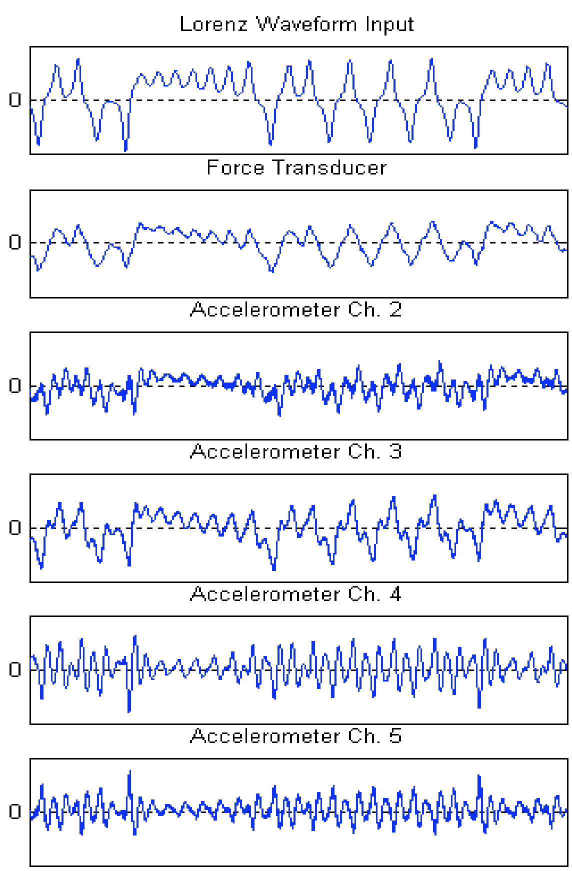

Figure 7. Representative time series responses for baseline conditions (damage case 1) illustrate how the structure successively filters the input signal that is propagated throughout the frame.

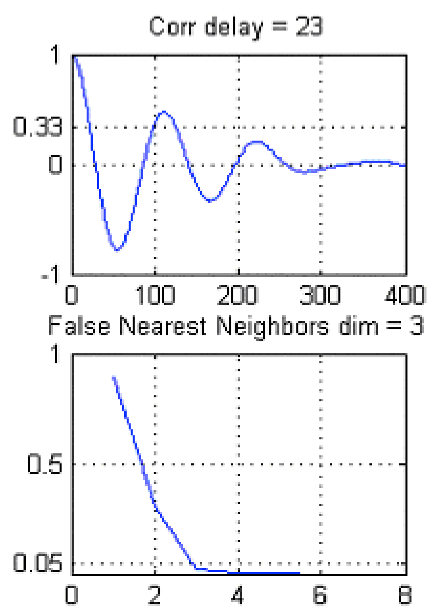

Figure 8. Representative auto-correlation and false nearest neighbors plots for determining delay and embedding dimension

IV. Results

Figure 9 shows the mean resampled prediction error between channel four and five, plotted against damage level. Examining the plot from tightest to loosest condition, there is an increase in the mean prediction error as the damage level makes the transition from tight to loose conditions. The first five damage levels can be considered tight conditions and the last three can be considered loose. The magnitudes of the error bars are equal to the resampled prediction errors' confidence interval at the corresponding damage level.

The probability density functions (PDFs) illustrate why the confidence intervals in the plot tend to increase with damage level. Figure 10 overlays eight PDFs that were generated using a kernel smoothing method from MATLAB. The PDFs corresponding to tight conditions are clustered on the left side of the plot while the loose condition PDFs are wider curves on the right.

Unfortunately the extent of the damage could not be seen. This limitation could be caused by the fact that the structure was not supporting a load except for its own weight. If the frame bears a load, the prediction error might be made more sensitive to subtle changes in the system dynamics. Loading the structure could allow the extent of the damage to be determined. Thus the correlation between bolt preload and attractor prediction error needs to be studied further.

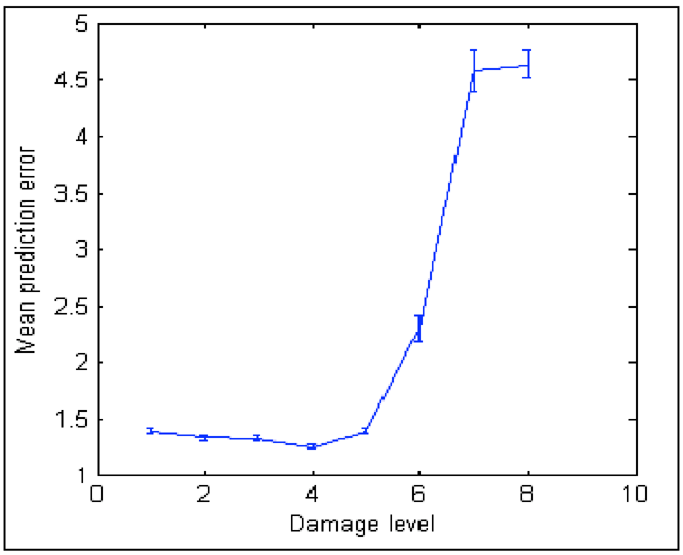

Figure 9. Mean prediction error of channel 4 predicting channel 5.

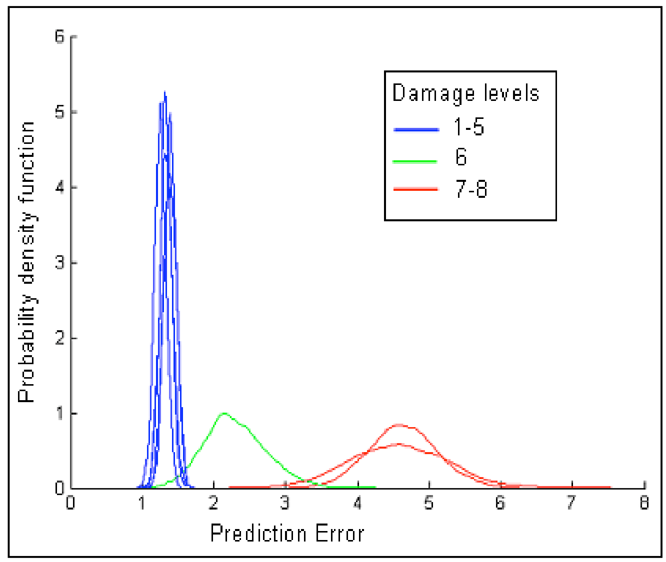

Figure 10. Probability density functions of prediction errors per damage case for channel 4 predicting channel 5.

The plots on Figure 11 indicate that the prediction error calculation is insensitive to forecast horizon. On each plot, the like colored lines correspond to prediction errors with five and ten time steps. The lines tend to track each other, pointing to insensitivity in the prediction error calculation to the number of time steps that the attractor trajectories are evolved.

Figures 9, 11, and 12 all indicate that this method cannot differentiate among tight conditions. In many cases, the mean prediction error at a given damage level is within the confidence limits of the mean at adjacent damage levels. Furthermore, Figures 11 and 12 indicate that locating damage with this technique may not be as straightforward as hoped. The prediction errors in the left hand plot in Figure 11 show an increase in prediction error in the Ch 1 to Ch 4 and Ch 1 to Ch 5 pairings as the bolt goes from tight to loose conditions. In addition, the prediction errors from Ch 1 to Ch 2 and Ch 1 to Ch 3 decrease under the same conditions, so it can be qualitatively concluded that the most decoupling of dynamic behavior takes place near the Ch 4 and Ch 5 accelerometers. It is known from the experimental set-up that was in fact the case. Other cross-prediction combinations (Figure 12) do not indicate that the prediction error from Ch 4 to Ch 5 stands out compared to other channel combinations that were not as close to the damaged location.

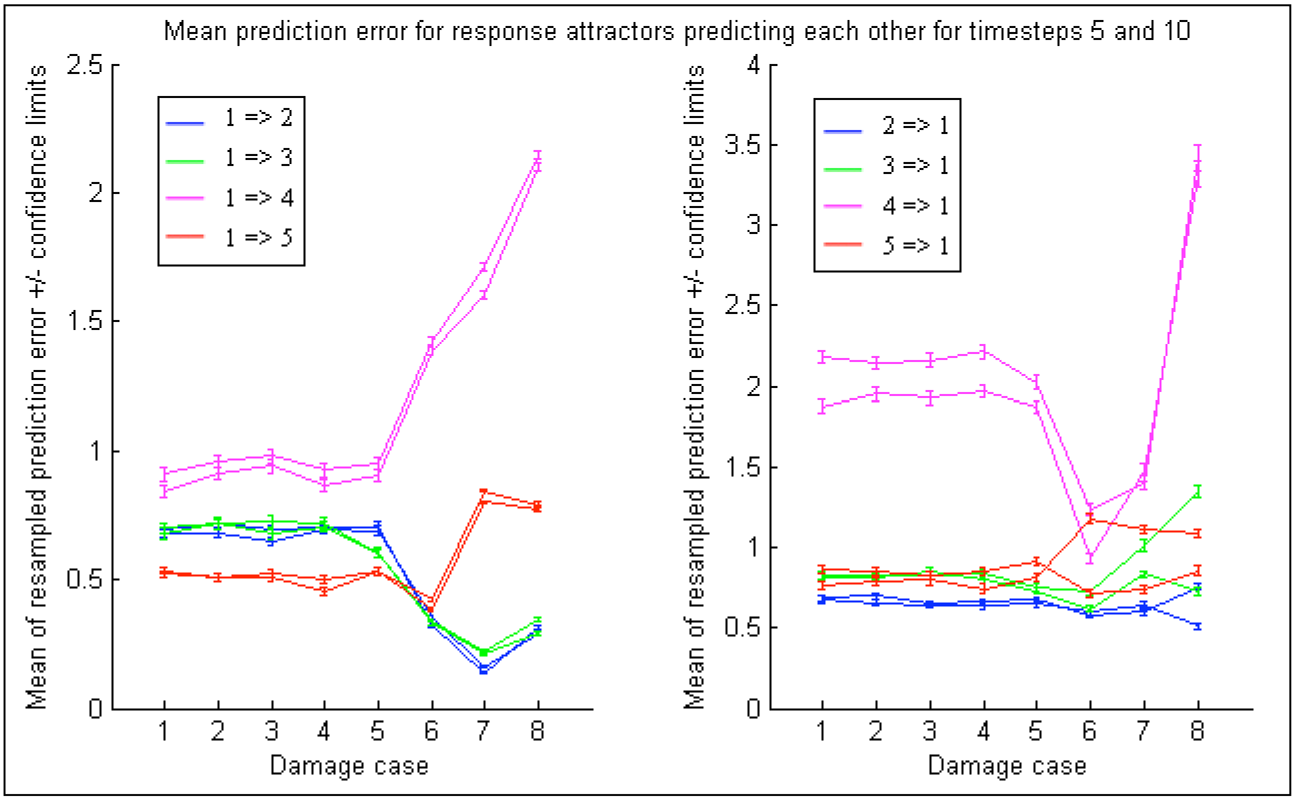

Figure 11. Average cross prediction error as a function of damage case for excitation (channel 1, force transducer) predicting the response (channels 2-5, accelerometers) and vice versa.

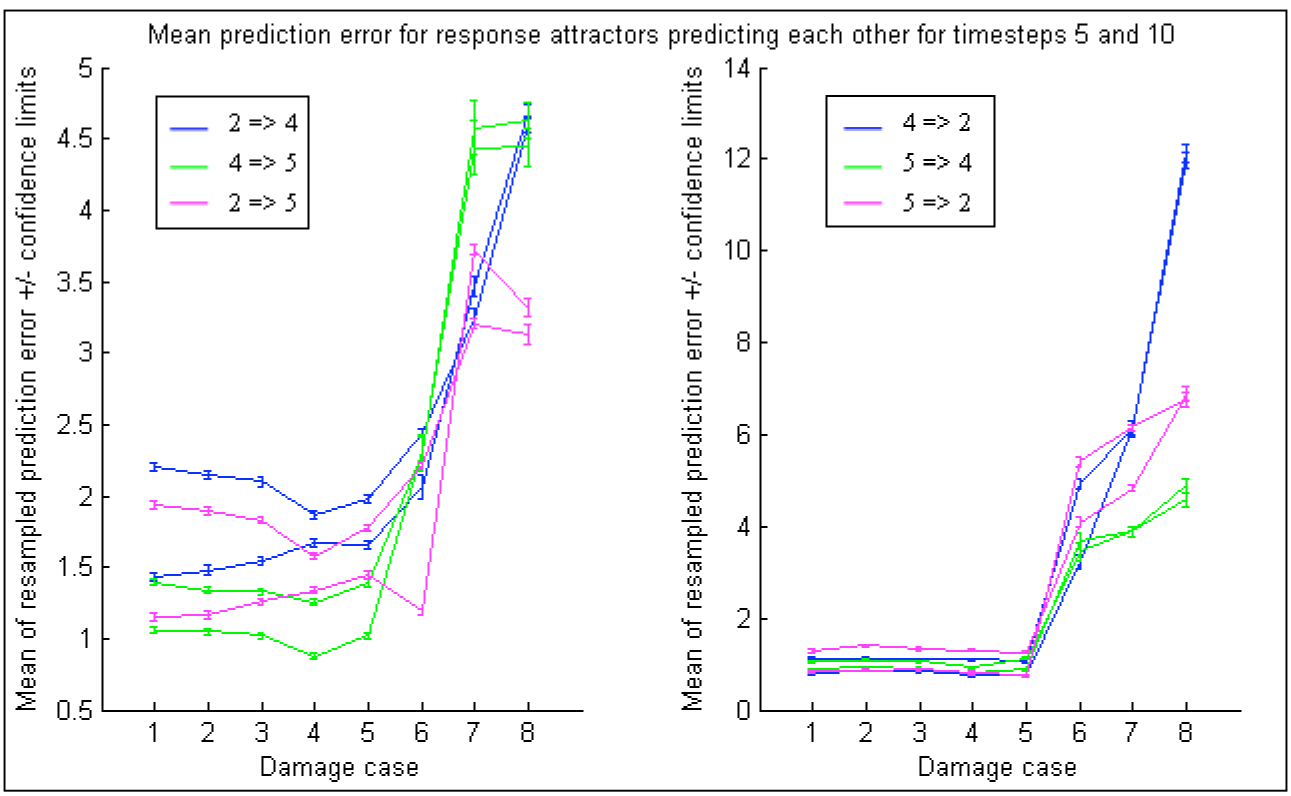

Figure 12. Average cross prediction error as a function of damage case for accelerometer responses at various locations predicting each other in both directions.

V. CONCLUSIONS

The cross prediction errors showed differences among damage conditions in a range from the 1 N-m of torque to sub-finger tight cases. Also, a qualitative examination of the prediction error trends for the force transducer predicting the accelerometer responses indicates that the damage location was between accelerometers four and five. However, the extent of the damage could not be determined because the prediction error was essentially the same value on the interval between the 27 N-m and the 1 N-m of torque cases.

For further research, an instrumented bolt more sensitive to the loads at the transition region is needed. Changes in parameters such as bolt preload, the rate of the chaotic waveform input, relative orientation between the shaker and the instrumented bolt, multiple damage points, and the locations of the accelerometers may be interesting for further study. Additional research could also investigate the effectiveness of this method for detecting damage in other modes of failure such as crack growth and weld unzipping.

VI. ACKNOWLEDGMENTS

The authors would like to acknowledge a number of individuals and organizations, without whose support this project would not have been possible. Chuck Farrar, of Los Alamos National Laboratory (LANL), hosted the Los Alamos Dynamics Summer School program, which sponsored this research project. Jonathan Nichols, from the Naval Research Laboratory, provided advice for data processing using time series analysis. Matt Bement and Jeannette Wait, both on LANL staff, helped with setting up data acquisition software and instrumentation. Special thanks to The MathWorks, Inc., for their generous donation of the MATLAB® 6.5 software used for computation.

Funding was provided by the Department of Energy and LANL. Our summer school work also made use of ABAQUS\CAE donated by Hibbit, Karlsson, and Sorenson, Inc. and ME'ScopeVES donated by Vibrant Technologies.

REFERENCES

[1] Doebling S W, Farrar C R, Prime M B 1998 A Summary Review of Vibration-Based Identification Methods *Shock and Vibration Digest*, 205(5):631-645.

[2] Nichols J M, Todd M D, Wait J R 2003 Using state space predictive modeling with chaotic interrogation in detecting joint preload loss in a frame structure experiment *Smart Mater. Struct.* 12(2003):580–601.

[3] Nichols J M, Todd M D, Seaver M. 2003 Use of chaotic excitation and attractor property analysis in structural health monitoring *Physical Review* E 67:016209

[4] Todd M, Wait J R, Nichols J, Trickey S. 2003 Joint Damage Assessment Using Output-Only Chaotic Attractor Property Analysis, Proceedings of IMAC XXI: A Conference on Structural Dynamics.

[5] Nichols J M, Moniz L, Todd M D, Trickey S T, Seaver M, Nichols C J, Virgin L N. 2003 Detection of Fastener Preload Loss in a Hybrid Composite-to-Metal Bolted Joint, 4th Int. Workshop on Structural Health Monitoring, Stanford, California, Sep. 15-17, 2003.

[6] Strogatz S H 1994 *Nonlinear Dynamics and Chaos, With Applications to Physics, Biology, Chemistry, and Engineering* (Reading,MA: Addison-Wesley)

[7] Lorenz E N 1991 Dimensionalities of weather and climate attractors *Nature* 353:241-244

[8] Sauer T, Yorke J A and Casdagli M 1991 Embedology *J. Stat. Phys.* 65:579

[9] Takens F 1981 Detecting strange attractors in turbulence *Notes in Mathematics vol 898)* ed D A Rand and L-S Young (New York: Springer) 366–81

[10] Kantz H and Schreiber T 1999 *Nonlinear Time Series Analysis* (Cambridge: Cambridge University Press)

[11] Kennel M B, Brown R and Abarbanel H D I 1992 Determining embedding dimension for phase-space reconstruction using a geometrical construction *Phys. Rev.* A 45**:**3403–11

[12] Nichols J M and Nichols J D 2001 Attractor reconstruction for nonlinear systems: a methodological note *Math. Biosci.* 171:21–32

[13] Pascual M and Levin S A 1999 From individuals to population densities: searching for the intermediate scale of nontrivial determinism *Ecology* 80**:**2225–36

[14] Schreiber T 1997 "Detecting and Analyzing Nonstationarity in a Time Series Using Nonlinear Cross Predictions" *Physical Review Letters* 78(5):843-846

[15] Hegger R, Kantz H, Schreiber T 1999 *Practical implementation of nonlinear time series methods: The TISEAN package*, CHAOS 9:413